

Influence of Weak Ground Ahead of the Tunnel Face on 3D-displacement and Face Extrusion

막장전방의 연약층이 터널 3차원변위 및 막장 수평변위에 미치는 영향

Jeon, Je-Sung*

전 제 성

요 지

터널시공 중, 터널자체의 안정성 확보와 주변지반 및 인접 구조물의 안정성 확보를 위한 체계화된 제측관리는 매우 중요한 사항이라고 할 수 있는데, 지반조건이 불리한 도심지 터널공사나 지반조건이 급격하고 빈번하게 변화하는 경우에 있어서는 그 중요성이 더욱 증대되는 것이 사실이다. 최근 오스트리아에서는, 임의 시점에 대한 절대변위를 계측하고 분석하는 기존의 방법대신, Geodetic을 이용한 각 시공단계별 상대변위의 계측 및 분석방법이 널리 증가하고 있는데, 이를 통해 지반조건이 급격한 변화 예측 및 이에 상응하는 굴착방법과 지보방식의 변경등이 용이해지고 있다. 한편, 지반의 변위는 막장 굴착이 시공되기 이전부터 발행하기 시작하므로 막장 전방의 응력상태는 향후 변위 진행과정에 있어 매우 중요한 요소라 할 수 있다. 즉, 막장 전방의 강성이나 응력상태는 굴착 후의 장기적인 터널안정성 및 인접 구조물의 안정성 확보와 관련된 주요 변수라 할 수 있다. 본 논문에서는 이와 관련된 다양한 조건에 대한 3차원 변위해석을 실시하였으며, 그 결과를 통해 터널 굴착시의 수직변위 및 벡터회전, 막장면 변위 등의 변화를 살펴보았다.

Abstract

During tunnel excavation in urban area a systematic monitoring is important for the purpose of determination of support type and quantity, as well as for the control of stability of both surface structures and the tunnel itself due to the frequently, and in many cases, abruptly changing ground condition. In Austria absolute displacement monitoring methods have replaced relative displacement measurements by geodetic methods to a large extent. Prompt detection of weak ground ahead of the tunnel face as well as better adjustment of excavation and support to the geotechnical conditions is possible with the help of the improved methods of data evaluation on sites. Deformation response of the ground to excavation starts ahead of the tunnel face, therefore, the deformation and state of the tunnel advance core is the key factor of the whole deformation process after excavation. In other words, the rigidity and state of the advance core play a determining role in the stability of both surface structures and the tunnel itself. This paper presents the results from detailed three-dimensional numerical studies, exploring vertical displacements, vector orientations and extrusions on tunnel face during the progressive advancement for the shallow tunnel in various geotechnical conditions.

Keywords : 3D displacement, Numerical analysis, Tunnel face extrusion, Vector orientation

1. Introduction

Tunnel construction in urban areas is difficult work

due to the lack of geological and geo-mechanical information of the ground to be tunnelled because of uncertainties with the local ground condition. Systematic

* Member, Doowoo Construction Engrg., Com., G. Manager, jesungjeon@hanmail.net

monitoring and interpretation of monitoring data to verify design parameters, quality control, and observation of the effectiveness of construction methods, etc. are important features of NATM. In the past during tunnel excavation on most sites, displacements of the tunnel have mainly been measured by tape convergence meters, extensometers, and leveling of roof points.

Interpretation of this data has been limited to a few observations of displacement graphs. This visual examination of graphs has a number of shortcomings (Schubert et al., 2002) and extensive research related to the monitoring and interpretation methods has been conducted to acquire better information for safety, stability and economic efficiency during tunnel excavation. Although the general geological situation may be known by site investigation and continuous monitoring of displacement graphs are made during the tunnel excavations, abrupt changes of ground conditions ahead of the tunnel face, which can cause serious damage to surface structures and the tunnel itself cannot be easily predicted with sufficient accuracy.

This paper presents the results of 3D numerical simulations carried out to evaluate spatial displacement and tunnel face extrusion in various situations for detecting changes of ground conditions and evaluating the stability in shallow tunnelling.

1.1 Vector Orientation, α

During the last decade, monitoring techniques and additional methods of evaluation have been improved in Austria using geodetic methods with 3D data. In geodetic methods, the measurement of absolute spatial displacements during tunnel excavation has become very common, replacing the previously used convergence measurements (Schubert et al., 1998, 2002). In Austria, observations on sites, where 3D displacements were measured, showed that the rock mass condition significantly influences the orientation of displacement vectors in space. When systematically evaluating the vector orientation of L/S (the ratio between longitudinal displacements and vertical settlements, Fig. 4), it was found that deviations from the

“normal” vector orientation indicate zones of different stiffness ahead of the tunnel face (Schubert and Budil, 1995) while the trend of crown settlement does not show any indication of the changing ground condition ahead of the tunnel face.

When a tunnel in relatively competent ground is approaching weak ground, stress concentrations on stiffer ground develop. In this case, the deviation of the principal stress direction tends to go against the excavation direction, increasing the longitudinal displacement, which also leads to an increase of α . In case of approaching stiffer ground, the opposite tendency occurs, i.e. the deviation of the principal stress direction tends to go toward the excavation direction with decrease of α .

Extensive numerical approaches have been conducted to confirm the observed phenomenon on sites and predict the existence of weak zones ahead of the tunnel face using the 3D boundary element method. The numerical results showed that the evaluation of the displacement vector orientations could provide valuable information on changes in rock mass quality ahead of the tunnel face.

Previous efforts on numerical approaches have been largely focused on deep tunnel with assuming linear elastic material. It is important to note, however, that the elasto-plastic material behavior of the ground, which causes stress redistribution and concentration near the tunnel face, is an essential factor in a shallow tunnel because the plastic zone around the underground opening considerably influences tunnel deformations and surface settlements.

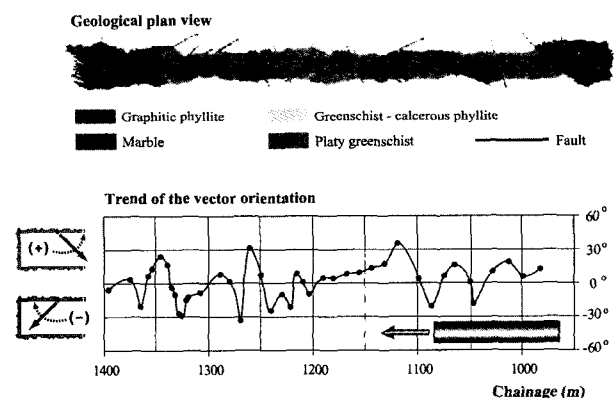


Fig. 1. Geological situation and trend line of the vector orientation at “Hinterberg” fault zone

1.2 Tunnel Face Extrusion

It was noted that the deformation response of the ground to be excavated starts ahead of the tunnel face and it produces a disturbance in ground, both in a longitudinal and transverse direction, which changes the original stress state. The effect of the disturbance caused by excavation corresponds to the formation of the channeling zone around the opening. This is related to the arch effect.

There have been remarkable research results from the ADECO-RS approach (Lunardi, 2000), in which deformations on the tunnel face are useful indicator to evaluate the ground response. This has been conducted in Italy over the last 25 years. In this approach, deformations caused by excavation are classified as preconvergence, convergence at tunnel circumference and extrusion (Fig. 2) which is the maximum longitudinal displacement at tunnel face. The main concept of this approach is that the stability of face advance core system plays a fundamental role in the deformation response of tunnelling in both the long and short term. In other words, as opposed to traditional NATM derived approaches, which consider only deformation that occurs in the tunnel behind the face, this approach studies the deformation response from the moment it begins ahead of the face as well as in the tunnel because deformation develops in the form of extrusion at the tunnel face, preconvergence and then finally convergence. Particular attention is paid to the behavior of the tunnel face and not just the inside of the tunnel, which is normally done.

Deformation response of the ground is illustrated as elastic behavior, elasto-plastic behavior and collapse of the ground opening with deformation on tunnel face (Fig. 2). P. Lunardi (1999, 2000) has studied possible connections between the deformation of the face advance core system and radial deformation of the tunnel behind the face. The first can be expressed as extrusion and preconvergence, and the latter can be expressed as convergence.

The results of research by monitoring on many sites and experiments showed that an arch effect related to tunnel stability has already been formed ahead of the

tunnel face and the deformation of the tunnel advance core was the true cause of the whole deformation process (i.e., extrusion, preconvergence and convergence). There are close connections between the failure of the advance core and the collapse of the ground opening, i. e., the rigidity and state of the advance core played a determining role in the stability of a tunnel both in the long and short term (Lunardi, 2000). Also, the state of the advance core can be illustrated by deformation of the tunnel face, i.e., extrusion.

Moritz et al. (2002), by experience gained at monitoring of a shallow tunnel under the Westbahn in Austria, reported that a key element in controlling the settlements appeared to be the enhanced support at the tunnel face which becomes evident from the correlation between number of face subsections and number and length of face bolts to the reduction of settlements ahead of the tunnel face. In other words, the additional measures for face stabilization had a very positive impact on displacement behavior both in the tunnel and at surface. From these results, it is worth noting that extrusion can be a good indicator for predicting the behavior in both tunnel and ground.

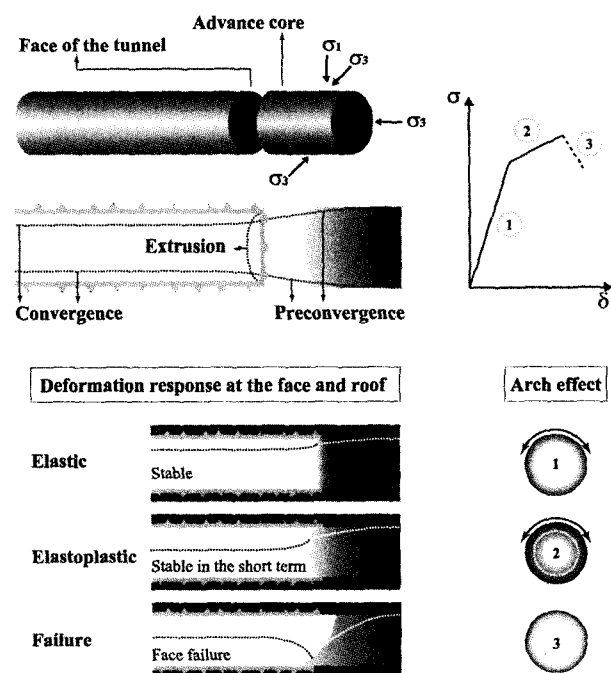


Fig. 2. Definitions of deformations and behavior of face advance core and tunnel roof

2. Numerical Model

2.1 Three-dimensional Finite Difference Models

The advancing process of a tunnel, which essentially has a 3D nature, has been studied by various authors who introduced different hypotheses in order to reduce it to a simpler 2D-scheme (Gioda et al., 1999). Several approximations have been suggested for including 3D effects in 2D analyses. The most common approximations used are the stiffness reduction (Laabmayr, 1986) and the load reduction methods (Panet, 1982), respectively. Plane strain models in 2D analyses, however, are only able to evaluate displacements and stress at some distance from the tunnel face and cannot account for stress redistributions, excavation sequencing and displacements ahead of and in the vicinity of the tunnel face (Pane et al., 1988; Kielbassa et al., 1991). Also, it is hard to account for the effect of faults and non-homogeneous ground conditions ahead of the tunnel face. To evaluate spatial displacements in tunnelling only 3D models are applicable.

Extensive 3D boundary element analyses to investigate the influences of various ground conditions ahead of the tunnel face (Steindorfer et al, 1998; Tonon et al., 2000) were conducted by assuming the ground is a linear elastic material on deep tunnel. It is worth noting that finite element or finite difference methods are most suitable for shallow tunnels in soil or weathered rock where the boundary element and discrete element methods are suitable for deep tunnels in jointed and faulted rocks at an angle (Schweiger et al., 1996). A series of three-dimensional finite difference models were constructed to investigate the influence of the existence of a weak

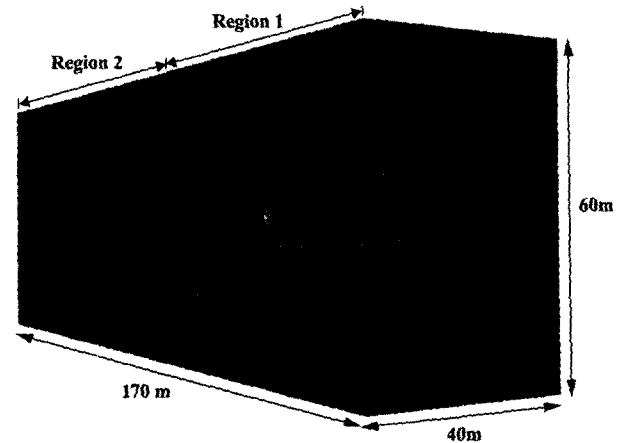


Fig. 3. Three-dimensional finite difference model and geometry

ground ahead of the tunnel face and solved by using the commercial code $FLAC^{3D}$. The model consists of 13,770 brick elements assumed to be symmetric in a parallel to the tunnel axis with a total length of 170m (Fig. 3). Some calculations having different model sizes were carried out to acquire sufficiently accurate results. The circular tunnel has a diameter of 10m with an outer boundary extending to a distance of 40m perpendicular to the tunnel axis and 30m to the vertical axis to minimize boundary effects. The models are divided into two regions (region 1 and region 2) having different geotechnical properties to simulate progressive excavation of the tunnel through the two regions. In the basic model (Fig. 3), region 1 and region 2 illustrate relatively stiff and weak ground, respectively.

The initial stress state corresponds to gravitational loading (Table 1) to simulate a shallow tunnel in an urban area. For each step the excavation is advanced 2.0m and support pressure is applied at specific distances from the tunnel face. In each case, analysis conditions and their

Table 1. Geotechnical properties used in 3D numerical simulations

Intact rock strength σ_{ci} (MPa)	Geological Strength Index GSI	Rock mass strength σ_{cm} (MPa)	Deformation modulus E_m (MPa)	Cohesive strength c (MPa)	Friction angle ϕ ($^{\circ}$)	Density ρ (kg/m 3)	Poisson's ratio ν	Classification
30	33	3.6	2,000	0.40	38	2,400	0.30	A $_1$
30	21	2.5	1,000	0.30	33	2,400	0.30	A $_2$
10	18	0.75	500	0.15	27	2,100	0.35	P $_1$
10	7	0.36	200	0.09	22	2,100	0.35	P $_2$
			100	0.05	20	2,100	0.35	P $_3$
			50	0.005	30	2,100	0.35	P $_4$

purposes are illustrated in more detail in later sections.

2.2 Analysis Methodology

Numerical simulations were carried out to investigate the variation of vector orientation, α , displacements (both in the vertical and longitudinal directions) and face extrusions with various cases when the tunnel face is advancing towards weak ground, from region 1 to region 2 (i.e. tunnelling is assumed to proceed horizontally from region 1 to region 2). Several influences such as: ground material (linear elastic or elasto-plastic), k_0 value, the stiffness ratio between the two regions, the length of the relatively weak ground, tunnel diameter, interface of stiffness transition between the two regions at an angle and non-homogeneity of geotechnical properties are considered in the numerical simulations.

Table 1 provides the geotechnical properties used in a series of numerical simulations with 3D finite difference models in both linear elastic and elasto-plastic materials. These are chosen for a typical weathered rock mass, weak

rock mass and soil derived from the generalized Hoek-Brown failure criterion.

Numerical analysis results encompass the total deformation process, including the displacement from the “undeformed” condition, until the excavation is finished and final equilibrium is obtained.

Monitoring data in the field, however, only shows certain portions of the total displacement because monitoring systems are installed after the excavation at a distance from the tunnel face. A certain amount of displacement has already taken place prior to start time of monitoring. Therefore, we should always take the zero reading at the same distance behind the tunnel face. To plot the numerical results of vector orientations (α) with the tunnel excavation process, ΔL and ΔS were calculated at each excavation step (Fig. 4).

3. Numerical Simulations

3.1 Influence of Relatively Weak Ground Ahead of the Tunnel Face

The first basic series of simulations were carried out to investigate the influence of the existence of the weak ground in tunnelling using geotechnical properties A_2 and P_3 shown in Table 1 for region 1 and region 2, respectively. The k_0 value is 0.5 in both regions.

Fig. 5 shows the trend of total displacement and typical displacement history with tunnel face advancement at the tunnel crown. Total vertical settlements in Fig. 5(a) were calculated 4m behind the tunnel face without zero reading. The results shown in Fig. 5(a) indicate that for existence of the weak ground (region 2) ahead of relatively stiff ground (region 1), there is no special increase in total vertical settlement until tunnel goes to $0.4D$ from the beginning of the weak ground. At distance greater than $0.6D$ (i.e. 6m) from the transition, total vertical settlements increased by 3.2cm. In practice, however, zero readings are taken at some distance behind the tunnel face because monitoring data show only a portion of the total deformation.

Fig. 5(b) provides displacement history familiar to most

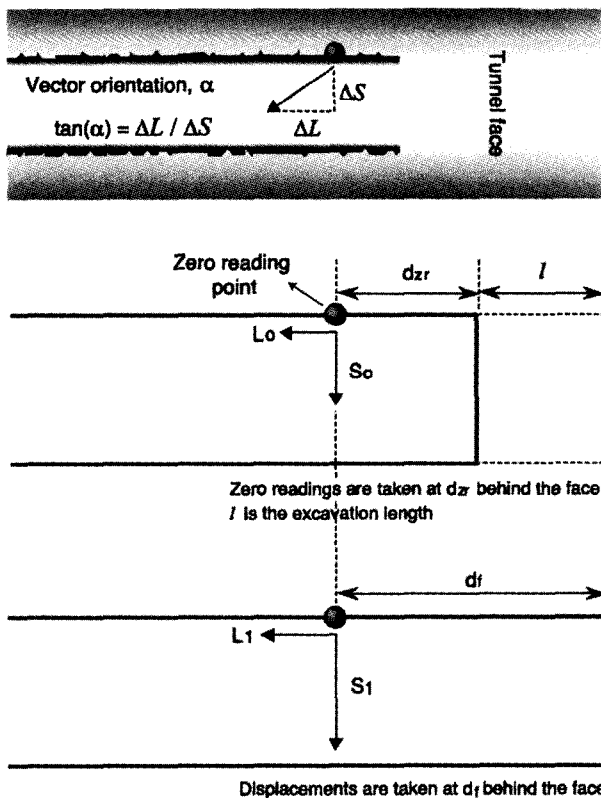
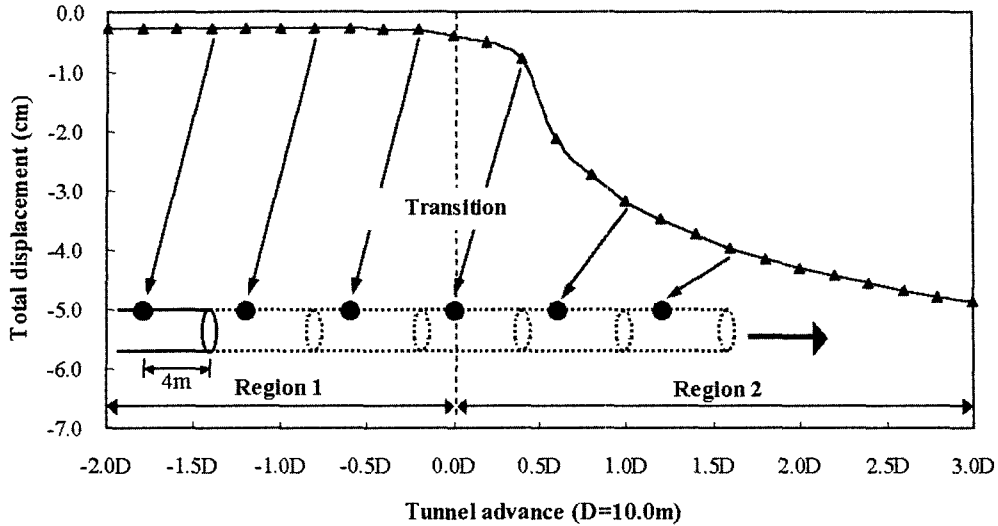
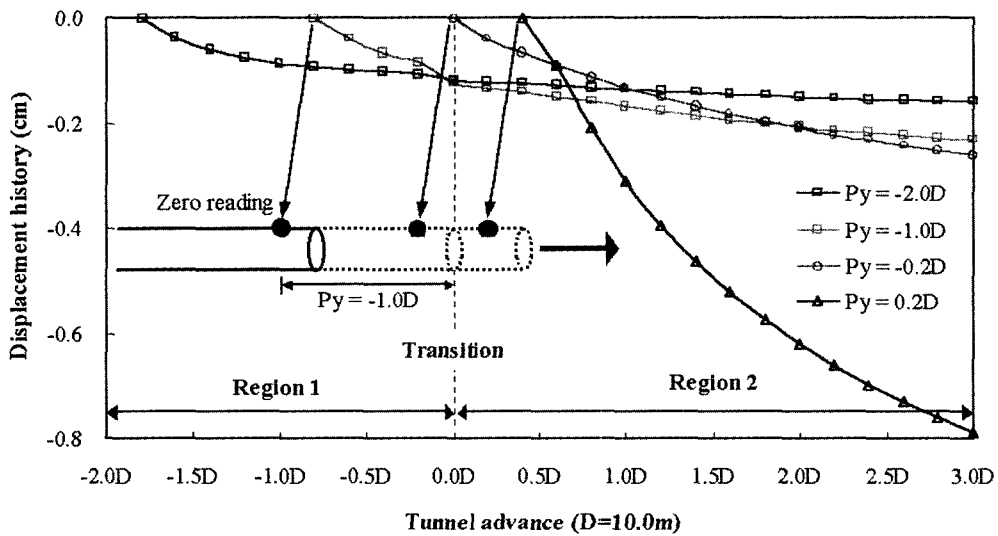


Fig. 4. Definition of the vector orientation (α) and zero reading



(a) Total vertical settlement 4m behind the tunnel face after zero reading 2m behind the tunnel face



(b) Vertical settlement history for fixed points

Fig. 5. Total displacement and typical displacement history with tunnel face advancement

tunnelling engineers. Fixed points for plots have been chosen at some distance ($P_y = -2.0D$, $-1.0D$, $-0.2D$ and $0.2D$) as shown in Fig. 5(b)) from the transition of adjacent two regions (i.e. region 1 and region 2). After zero readings have been taken 2m behind the tunnel face for a fixed point, increases of vertical settlements followed by tunnel advancement were calculated. At P_y (i.e. distance from the transition to fixed point for measuring) less than $0.2D$ (i.e. tunnel face is at $0.4D$), the displacement rate, which is used for predicting existence of the weak ground ahead of the relatively stiffer ground or evaluating the destabilization, has no special acceleration. Displacement rates begin to accelerate

as the tunnel face passes some distance in weak ground but the magnitude of displacement is smaller than the total displacement.

Accordingly, it can be seen that existence of the weak ground can't be recognized by displacement only until tunnel passes some distance in weak ground. It is also difficult to be sure of destabilization as tunnel advance in weak ground. How misleading this type of measurement data evaluation can be is shown in paper by Rokahr et al. (2002).

Fig. 6 shows a comparison between the trends normalized vector orientation, $\angle \alpha$, total vertical settlement and extrusion with tunnel advance. Up to the station $-2.0D$

(i.e. distance from the transition to tunnel face), no special changes in vector orientations are observed and this value is considered as average vector orientation, α_{ave} . Evaluation of data in the region 1 up to $-2.0D$ shows that average vector orientation, α_{ave} , is around -15° . Schubert et al. (1998, 2000) notes that average monitored angle between longitudinal displacement and crown settlement is between -8° and -12° from the evaluation of data taken from tunnels constructed in poor rock. In this paper, all vector orientations, α , are normalized by α_{ave} : normalized vector orientation $\Delta\alpha = \alpha - \alpha_{ave}$.

When the tunnel approaches weak ground, the relative

increase in longitudinal displacements is considerably higher than the relative increase in radial displacements. Therefore, with decreasing distance to the weak ground, $\Delta\alpha$ increases drastically although total vertical settlement has no special acceleration. It means that, by evaluating the vector orientation in tunnelling, changes in the ground condition can be predicted by several tunnel diameters ahead of the tunnel face. Also, the change in ground condition can be recognized much earlier when using vector orientations trend than by evaluating the vertical settlements only.

Fig. 7 shows plots of normalized vector orientation for

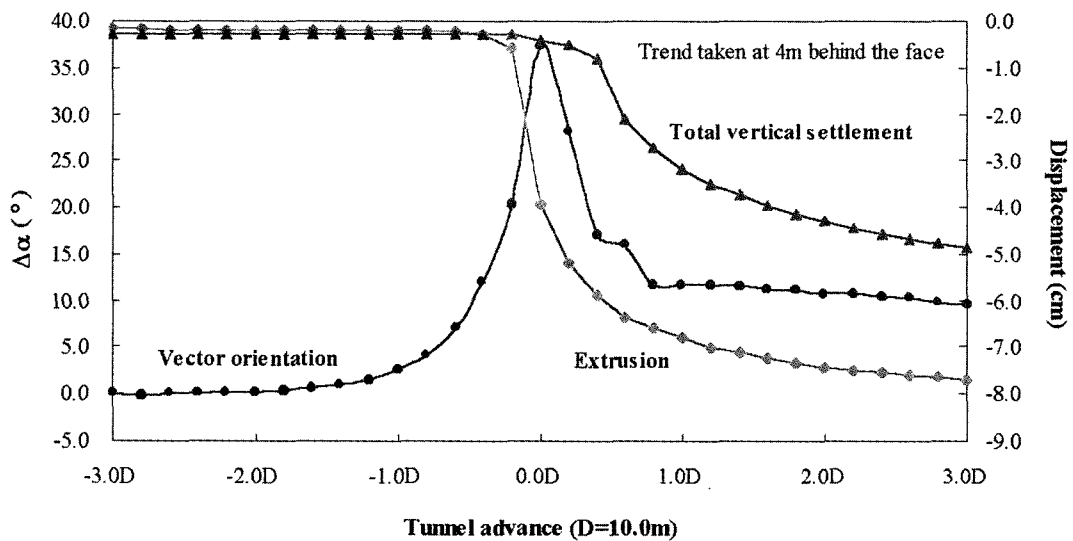


Fig. 6. Trend of displacement and vector orientation at crown with tunnel advance

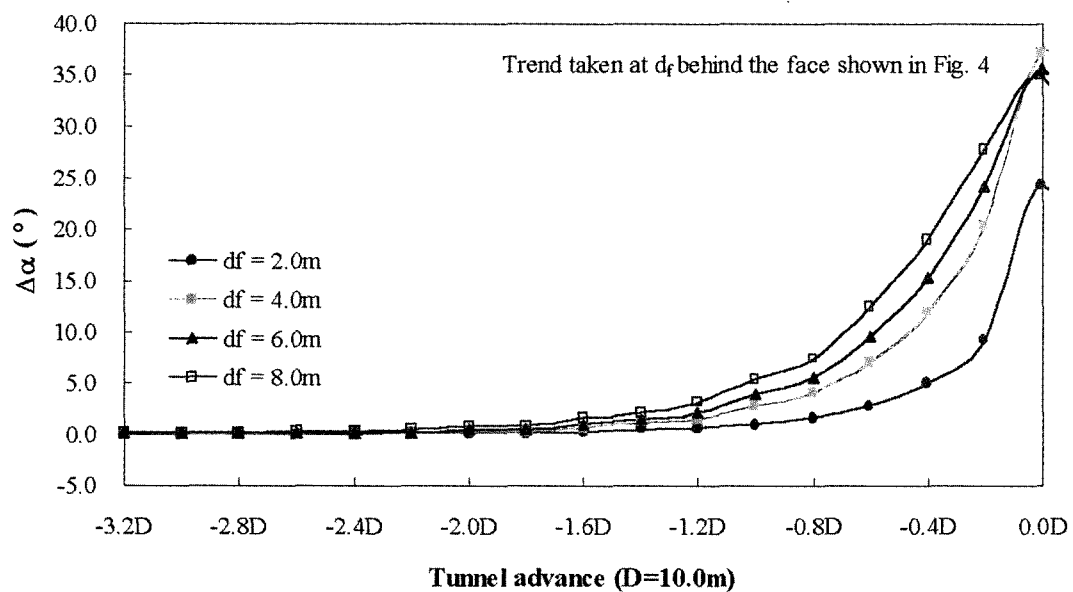


Fig. 7. Trends of $\Delta\alpha$ at the crown points 2.0m, 4.0m, 6.0m and 8.0m behind the tunnel face

each crown points 2.0, 4.0, 6.0 and 8.0m (i.e. $0.2D$ to $0.8D$ shown in Fig. 4) behind the tunnel face. Studies by Golser et al. (2000) notes that, the trend taken at further distance from the tunnel face, in elastic material, shows a larger deviation of the vector orientation than the trend near the tunnel face. In numerical simulations, we can confirm these effects easily when deformation response of the ground is elastic. However, in field, it's not easy to measure very small variation in longitudinal displacements at further point because of the measurement accuracy. Therefore, if we want to see the larger deviation of the vector orientations at further distance from the face, the amount of longitudinal displacements should be considerable. Also, if the plastic zone develops around the tunnel in elasto-plastic material, maximum deviation of the vector orientation is larger than elastic case.

With respect to trend of the extrusion shown in Fig. 6, it is of interest to note that acceleration of extrusion starts $-0.5D$ behind the weak ground with larger amount than the vertical settlements and longitudinal displacements at a distance behind the tunnel face.

3.2 Linear Elastic and Elasto-plastic Behavior

A big advantage of 3D finite element or difference analysis compared to that of 3D boundary element solutions is the ability to model elasto-plastic material

behavior. With elastic solution, regardless of whether ground is weak or stiff, the displacements are unlimited in terms of the magnitude they may reach and influences of the weak ground ahead of the tunnel face cannot be shown clearly. In real cases, however, the ground ahead of the tunnel face can yield as tunnel approaches the weak ground under the stresses resulting in a redistribution of the stress around the tunnel boundary. Panet (1993) notes that it is important to distinguish whether the plastic zone develops along the tunnel periphery behind the excavation face, or whether it encircles the excavation face thus endangering the stability of the face.

Mohr-Coulomb elasto-plastic constitutive relationship was used to model yield deformation for the simulations. A comparison between total vertical settlement at tunnel crown 4m behind the face and extrusion at tunnel face calculated assuming linear elasticity and elasto-plastic yielding are shown in Fig. 8 with the same geotechnical properties above. These results show that increases of the extrusion as tunnel approaches the weak ground in the elasto-plastic material are significantly larger than results in linear elastic material.

Referring to results of total vertical settlement in elasto-plastic and linear elastic material, there is no special difference until the tunnel goes to $0.6D$ (i.e. 6m) in weak ground. In case of elasto-plastic material, when the tunnel face is at $0.6D$, plastic zone extends appro-

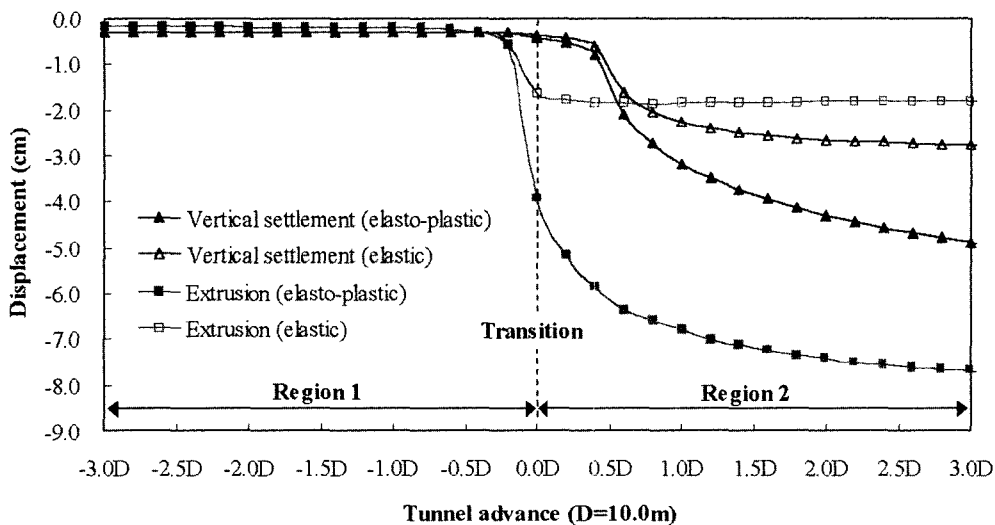


Fig. 8. Trends of the total vertical settlement and extrusion having different model at the crown points 4.0m behind the tunnel face ($k_0=0.5$)

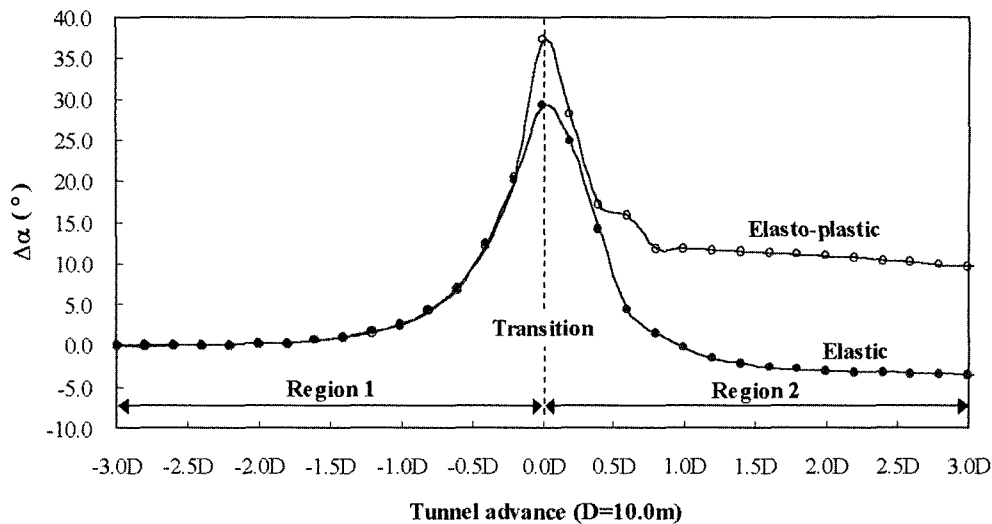


Fig. 9. Trends of $\Delta\alpha$ having different model at the crown points 4.0m behind the tunnel face ($k_0=0.5$)

ximately 5m and 8m in the direction of radial and longitudinal from the tunnel boundary, respectively (Fig. 10).

Lunardi et al. (1999, 2000) notes that the deformation response begins ahead of the tunnel face in advance core (Fig. 2) and develops backwards from it during tunnelling. They also, during experiments at the filed and laboratory, found that there is a close connection between the deformations (i.e. extrusion and preconvergence shown in Fig. 2) of the advance core ahead of the tunnel face and the convergence behind the tunnel face. It means that it is essential to reduce the deformation ahead of the tunnel

face for the short and long term stability of the tunnel. It is important to note that if the instability in weak ground is detected too late during excavation, a large plastic zone, which can be true cause of the further deformation after excavation, is already formed ahead of the tunnel face as shown in Fig. 10. Examination of normalized vector orientations in Fig. 9 shows that plastic behavior has only a minor effect with respect to deviating the vector orientation as tunnel approaches the weak ground although, in elasto-plastic model, the maximum deviation of $\Delta\alpha$ at the beginning of weak ground is a little larger than that of elastic model. Studies by Schubert et al. (1995, 1998, 2000) have shown that, with decreasing distance to transition, the deviation of the vector orientation from the normal value (i.e. vector orientation value in unaffected region by weak ground) starts at a distance ahead of transition, and then normalization of the vector orientation is observed again at the same distance after the transition. This result can be attributed to the limitations associated with assuming the linear elastic behavior and same Poisson's ratio, ν , for stiff and weak region in his studies. In real case, having different Poisson's ratio for each region in elasto-plastic material, vector orientation after transition does not converge to a same value of the average vector orientation, α_{ave} , in stiff region. The vector orientation depends on a couple of factors, like initial stress state, Poisson's ratio, rock mass structure and such like.

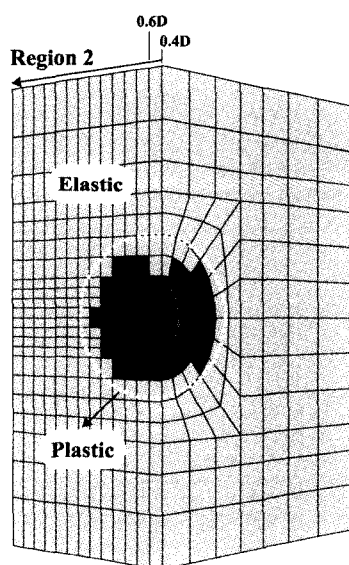


Fig. 10. Plots of the plastic zone around the tunnel face at 0.6D from the transition

3.3 In Situ Stress State

A series of simulations were carried out to investigate the influence of initial principal stress state using geotechnical properties A_2 and P_3 shown in Table 1 for region 1 and region 2, respectively. In each case, the initial vertical stress was assumed to be equal to the overburden load with the far-field horizontal stresses. In other words, different k_0 values (i.e. horizontal/vertical

stress ratio) were assumed ($k_0=0.5, 0.75$ and 1.0) in elasto-plastic material.

Fig. 11 provides plots of the total vertical settlement and extrusion trend until the tunnel reaches the weak ground (i.e. until station of the tunnel face is equal to $0.0D$) for each of the cases having different k_0 value.

In the results of the total vertical settlement shown in Fig. 11, when the tunnel face is at $4m$ ahead of transition (i.e. 0.4 tunnel diameter), difference of the magnitudes

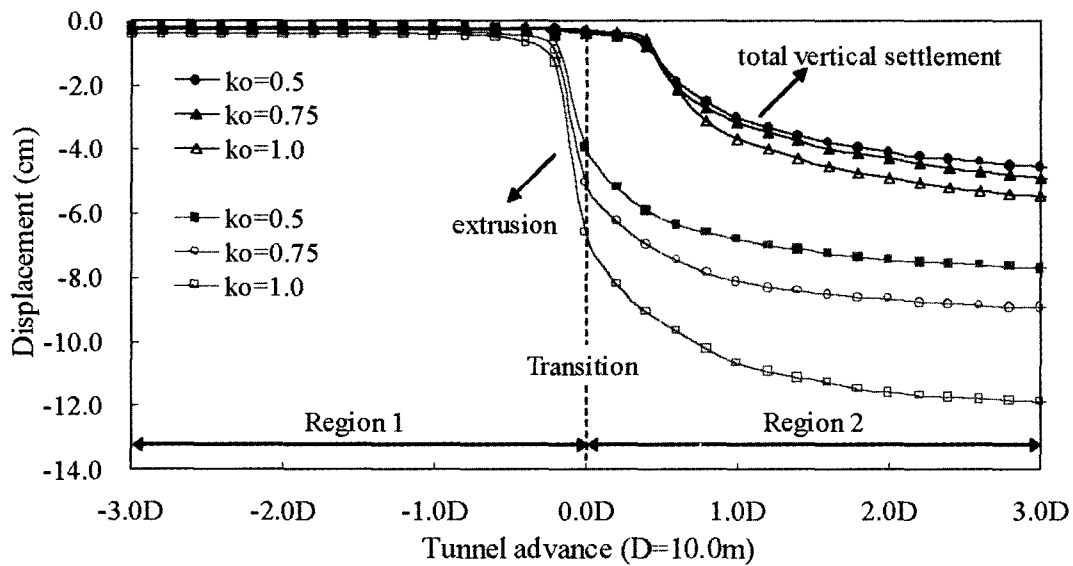


Fig. 11. Plots of total vertical settlement and extrusion having different in situ stress state (i.e. $k_0=0.5, 0.75$ and 1.0) at the tunnel crown $4.0m$ behind the face and tunnel face, respectively

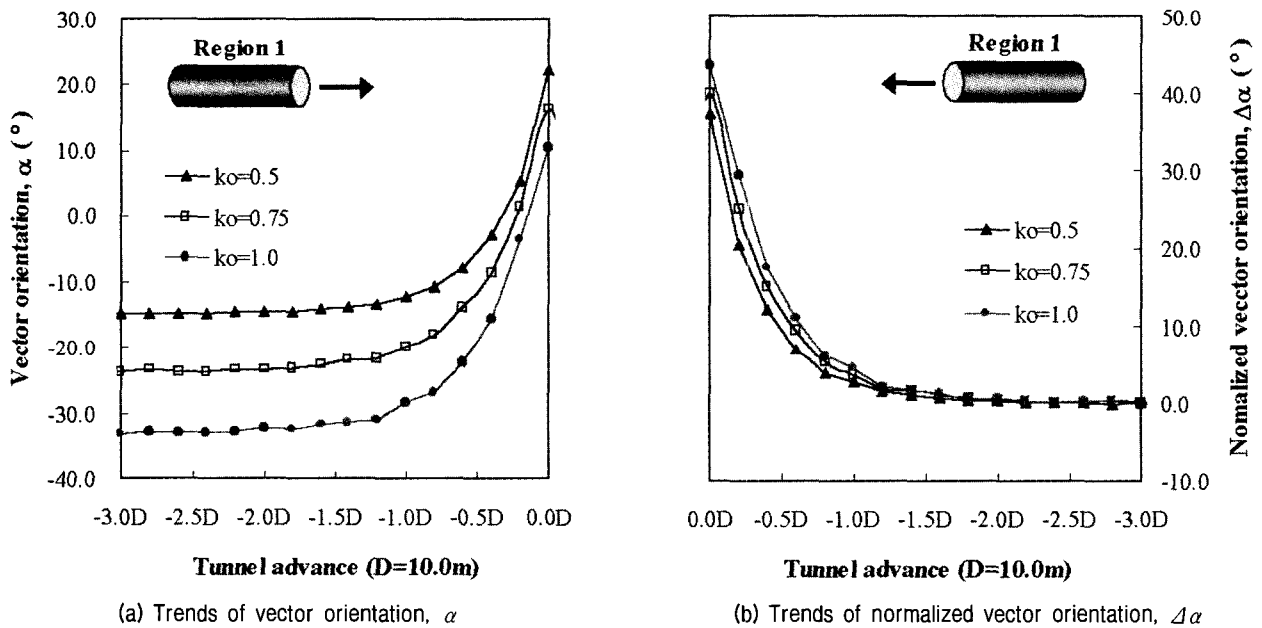


Fig. 12. Plots of vector orientation and normalized vector orientation having different in situ stress state as tunnel approaches weak ground in region 1

in the total vertical settlements varies from 0.05cm to 0.18cm with respect to k_0 , while extrusion shows a larger difference varying from 1.06cm to 3.18cm. In region 1, a large increase of extrusion starts 4m (i.e. -0.4D) behind the transition, while total vertical settlement has no special variations.

In the trend of the vector orientation shown in Fig. 12 as the tunnel approaches a weak ground, with increasing k_0 , the maximum deviation of the vector orientations from normal value become larger from 37° to 44° because for the high k_0 values the change in longitudinal displacements in the vicinity of the tunnel face is much higher than for small k_0 values. The variation starts a little earlier in spite of the fact it has only a minor effect with respect to k_0 value. With increasing k_0 , the vectors tend to point more against the direction of the excavation.

The results show a significant influence of the in situ stress state on the extrusion at the tunnel face to predict existence of weak ground ahead of the tunnel face and evaluate the tunnel stability when tunnelling, while the total vertical settlement and vector orientation at the tunnel crown are nearly unaffected. In the results of simulations assuming linear elastic behavior, trends of the vector orientation are nearly the same as above results.

3.4 Stiffness Ratio

To investigate the influence of the stiffness ratio, SR (i.e. ratio of elastic modulus of region 1 to region 2), different elastic modulus and strength parameters for regions were assumed. Table 2 summaries the geotechnical properties used in simulations with respect to the stiffness ratio adjacent two grounds. In addition, computed nor-

malized vector orientation 4m behind the tunnel face and extrusion at the tunnel face was provided in Table 2. The displacement measurements are taken at a distance 4m (0.4D) behind the tunnel face and k_0 used in all simulations is 0.5.

The results show that, with increasing ratio of stiffness between two regions, the maximum deviation of the vector orientation, $\Delta\alpha_{max}$, increased a little. In the case of assuming elasto-plastic behavior, however, it is hard to predict stiffness ratio between two regions in terms of the analysis of vector orientation only. As shown on Table 2, in Case III, IV, V and VI, deviation of the vector orientation seems to be similar before the tunnel face reaches the weak ground (i.e. station 0.0D) in spite of its different geotechnical properties. Although, in Case V, the failure occurred along the tunnel boundary followed formation of large plastic zone as the tunnel face approaches the weak ground, results of the vector orientation show similar trend as other case. In other words, trend of the vector orientation and vertical settlement only can't reflect instability of the ground with respect to accumulation of the plastic deformations, which initiate ahead of the tunnel face.

Results for the extrusion on the tunnel face are seen to vary as condition for simulation though it has same stiffness ratio because extrusion depends on the strength and deformation properties of the ground ahead of the face and on the original stress field to which it was subject.

3.5 Length of Relatively Weak Ground

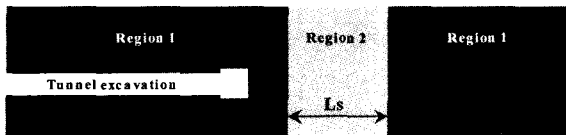
A series of numerical simulations have been conducted

Table 2. Geotechnical properties used in simulations, and computed vector orientation and extrusion

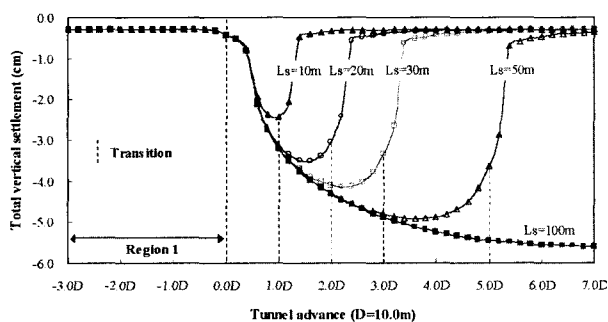
Case	Property classified in Table 1		SR E_1 / E_2	Normalized vector orientation, $\Delta\alpha^\circ$ at each station of the face				Tunnel face extrusion at each station of the face (cm)			
	Region 1	Region 2		-1.0D	-0.6D	-0.2D	0.0D	-0.2D	0.0D	0.4D	0.8D
I	A ₂	P ₁	2.0	0.85	2.24	5.93	14.33	0.27	0.39	0.41	0.42
II	A ₂	P ₂	5.0	2.00	5.32	14.46	30.51	0.43	1.32	1.67	1.77
III	A ₂	P ₃	10.0	2.71	7.00	20.40	37.17	0.57	3.95	5.88	6.61
IV	A ₁	P ₂	10.0	2.71	7.00	20.24	34.44	0.28	1.23	1.61	1.74
V	A ₂	P ₄	20.0	2.91	7.83	25.33	Failure	0.68	Failure	-	-
VI	A ₁	P ₃	20.0	2.91	7.83	25.18	39.03	0.34	3.75	5.79	6.57

to investigate the influence of the weak ground having different extensions shown in Fig. 13(a), i.e., $L_s=10$ (1.0D), 20 (2.0D), 30 (3.0D), 50 (5.0D) and 100m (10.0D).

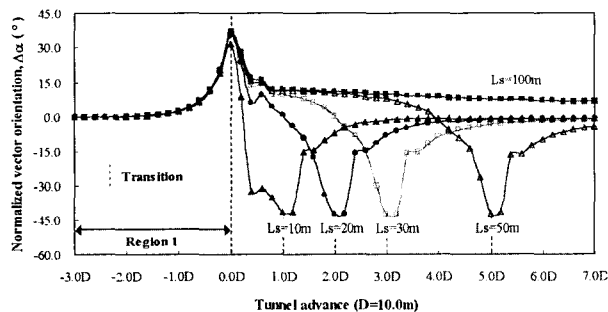
The results of total vertical settlement shown in Fig. 13(b) show that tunnelling behind weak ground does not



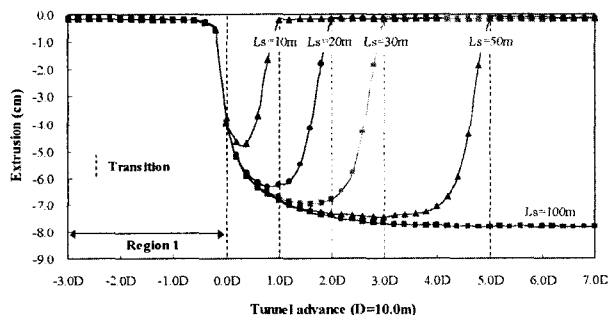
(a) Extension of the weak ground, L_s . Transition interface would be aligned perpendicular to the tunnel axis



(b) Trends of total vertical settlement with different L_s ($L_s=10$, 20, 30, 50 and 100m)



(c) Trends of normalized vector orientation, $\Delta\alpha$, with different L_s



(d) Trends of the extrusion on tunnel face with different L_s

Fig. 13. Plots of displacements and normalized vector orientation having different extensions of the weak ground (i.e. region 2), L_s , for trends taken at 4m behind the tunnel face and k_0 equal to 0.5

produce an increase in the settlements regardless of the weak ground's extension. In addition, the amount of total vertical settlement became smaller as the extension of the weak ground decreased. As a result, the numerical simulations show that the evaluation of trends of vertical settlement only, do not provide clear indication of weak ground or fault zone ahead of the tunnel face, because the increase of the absolute displacements may also be caused by a continuous increasing deformability of the ground.

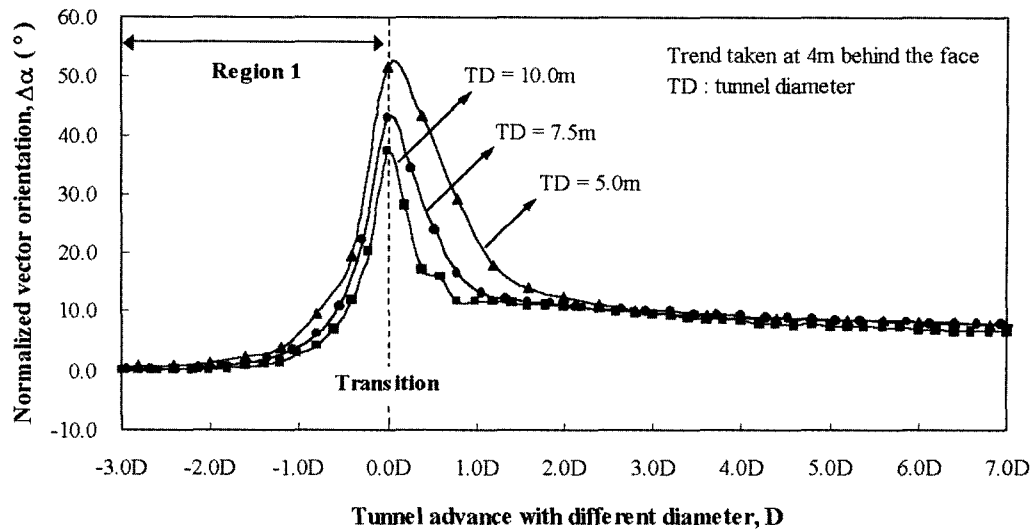
Fig. 13(c) shows the trend of normalized vector orientation. When the tunnel approaches the weak ground, the vector orientation showed an increasing trend against the direction of excavation. After the tunnel face entered the weak ground and approached the relatively stiff ground again, the vector orientation dropped down and recovered gradually. It is interesting to note that, regardless of the extension of the weak ground, the deviation of $\Delta\alpha$ starts at a similar distance behind the weak ground and the maximum deviations of $\Delta\alpha$ almost appear to be similar. In more quantitative terms, the difference of $\Delta\alpha_{\max}$ in cases of $L_s=10$ and 100m is less than 6° . Steindorfer (1998) notes that a certain prediction of the extension of a fault zone as well as zones consisting of relatively weak ground ahead of the tunnel face is possible with the analysis of the vector orientation trends, as shown in Fig. 13(c).

As described above, however, it depends on the amount of displacement in vertical and longitudinal direction as well as the initial stress state, Poisson's ratio, rock mass structure and such like. Therefore, it is not easy to predict the extension of the weak ground by $\Delta\alpha$ only in practice.

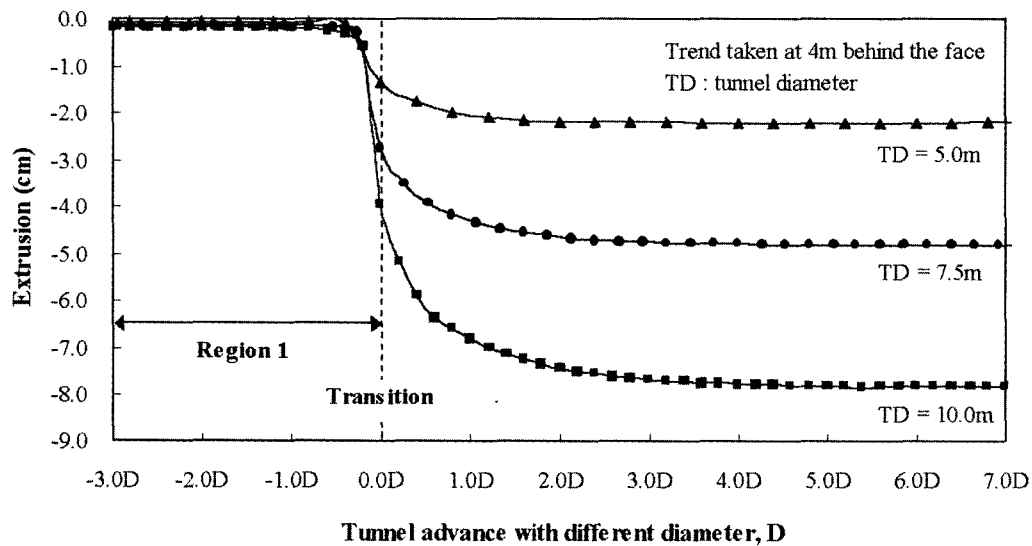
3.6 Tunnel Diameter

From the results of all simulations, the change in ground condition ahead of the tunnel face can be recognized at a distance from -2.0D to -1.0D behind weak ground when using vector orientation trend.

Various tunnel diameters were assumed to investigate the influence on displacements and vector orientation with diameter equal to 5.0, 7.5 and 10.0m in a same



(a) Trends of $\Delta\alpha$ having different tunnel diameter



(b) Trends of extrusion having different tunnel diameter

Fig. 14. Plots of vector orientation and extrusion having different tunnel diameter ($D=5.0, 7.5$ and 10.0m)

model boundary and geotechnical properties.

Tunnel was modeled at the centre of the model boundary. In each case, the initial vertical stress was assumed to be equal to the overburden load with $k_0=0.5$ in elasto-plastic material. Accordingly, in each case, initial stress conditions were not identical

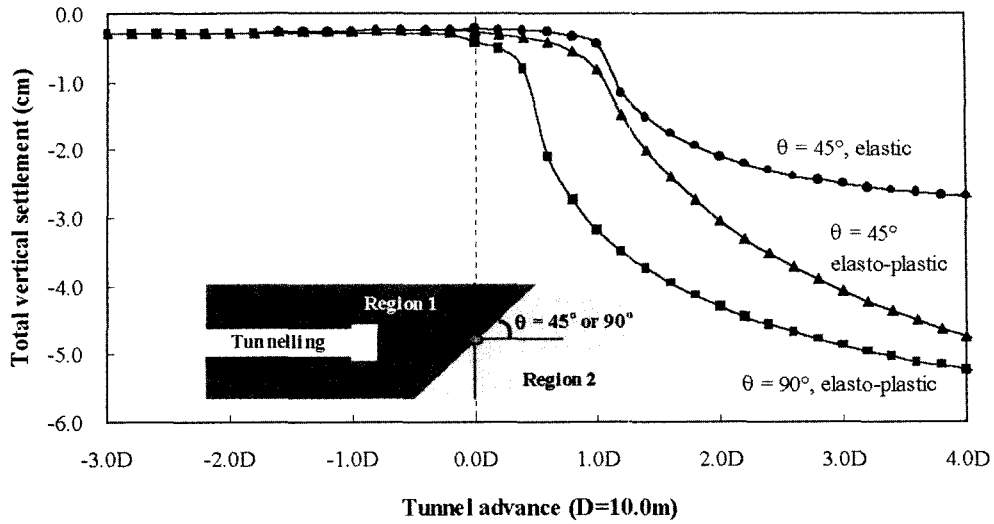
The results of the normalized vector orientation shown in Fig. 14(a) show that, with decreasing tunnel diameter, the maximum deviation of the vector orientation becomes larger and variation of the vector orientation starts a little earlier as opposed to common sense because for the small tunnel diameter the ratio of change in longitudinal displacements to vertical settlements in the vicinity of the

transition is a little higher than for large tunnel diameter. It is difficult to be sure, using results of vector orientation only, existence of weak ground ahead of the face and instability caused by weak ground in quantitative terms.

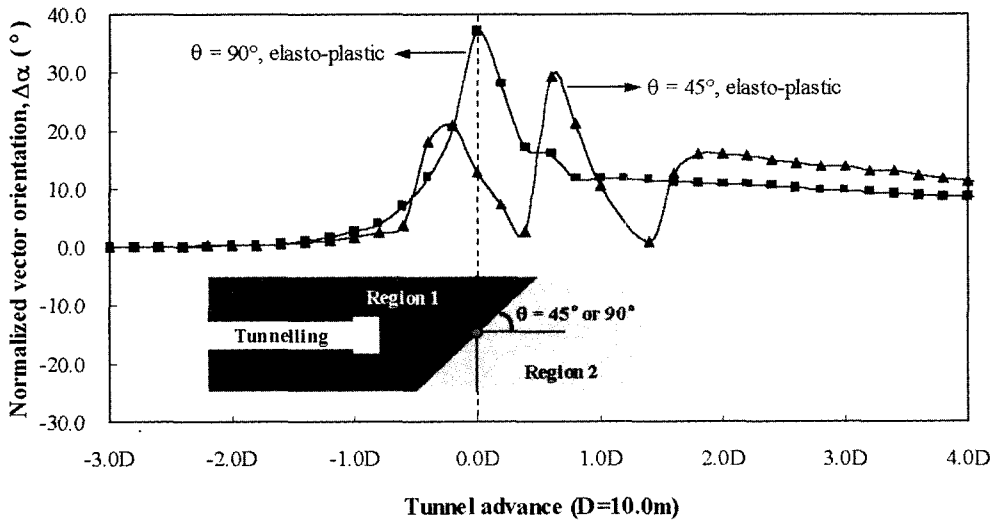
As opposed to the results of vector orientation, trends of extrusion with respect to tunnel diameter shown in Fig. 14(b) provide more clear indication for prediction of existence and instability of weak ground.

3.7 Interface of Transition at an Angle

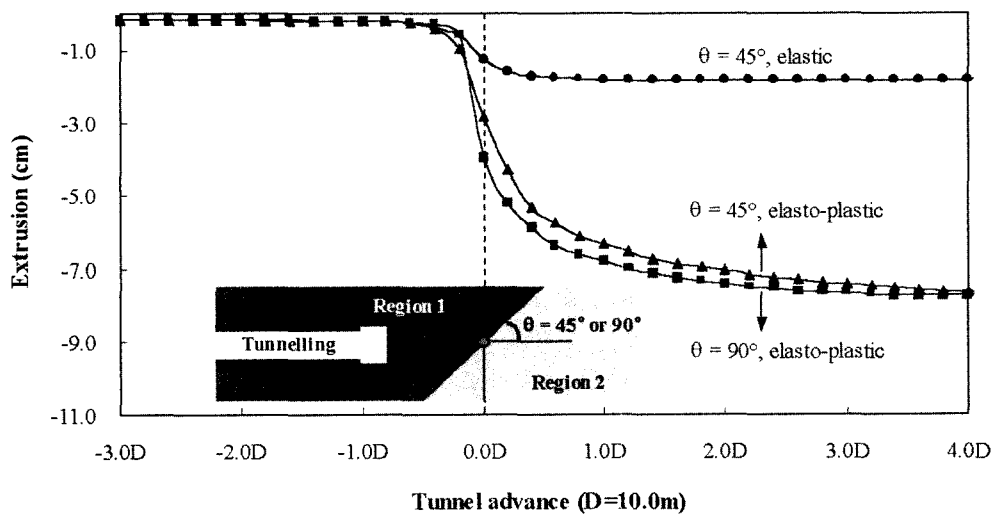
From the results of all simulations above, transition interface between two regions was aligned perpendicular



(a) Trends of total vertical settlement



(b) Trends of normalized vector orientation, $\Delta\alpha$



(c) Trends of extrusion at tunnel face

Fig. 15. Plots of displacements and vector orientation with the inclination of the transition interface sloped at $\theta = 45^\circ$ and 90° with respected to the tunnel axis, assuming elasto-plastic and elastic material

to the tunnel axis while, in practical case, the interface can be at an angle.

Numerical simulations were carried out with the inclination of the transition interface sloped at $\theta=90^\circ$ and 45° with respect to tunnel axis in elasto-plastic and elastic material. Geotechnical properties used in simulations are A_2 and P_3 shown in Table 1 for region 1 and region 2, respectively with $k_0=0.5$.

Comparisons between inclinations of transition interface assuming linear elastic and elasto-plastic yielding are shown in Fig. 15. Tunnel advances at the x-axis in Fig. 15 represent a distance from centre of the transition interface to centre of the tunnel face.

Results about total vertical settlement shown in Fig. 15(a) indicate that a certain amount of increase can be shown from 1.0D, 1.0D and 0.4D ahead of the transition in case of $\theta=45^\circ$ assuming elastic material, $\theta=45^\circ$ and $\theta=90^\circ$ assuming elasto-plastic material, respectively. In other words, when the transition interface is at an angle, vertical settlements can't provide valuable information for prediction of the existence of the weak ground ahead of the tunnel face as well as evaluation of the stability in both tunnel and ground even if the tunnel face is nearby the weak ground in which collapse at the tunnel face does not occur.

The changes of the vector orientation at the tunnel crown are shown in Fig. 15(b). It is interesting to note that there are huge differences between $\theta=45^\circ$ and 90° in elasto-plastic material for section near the transition. In case of $\theta=90^\circ$, the vector orientation deviates from the normal about one diameter behind the centre of transition interface and increased drastically as tunnel face approaches the transition. The maximum deviation of $\Delta\alpha$ is 37° when the tunnel face is at the transition.

In case of $\theta=45^\circ$, vector orientation begins to deviate from normal about 0.6 diameter behind the centre of transition interface and reaches the first peak value in region 1, $\Delta\alpha_{\max}=21^\circ$. When the tunnel face meets the centre of the transition interface, i.e. tunnel face is at 0.0D, the vector orientation shows decreasing tendency, while large deformation could occur as a result of elasto-plastic yielding. In addition, the vector orientation

fluctuates 3 times near to the transition interface. In aspect of practical use on sites, using measurement of vector orientation only such as the result shown in Fig. 15(b) assuming inclination of the transition interface, the result seems to make argument about the next rounds or additional support.

Fig. 15(c) shows the trend of extrusion on the tunnel face for the cases of $\theta=45^\circ$ in elastic material, $\theta=45^\circ$ in elasto-plastic material and $\theta=90^\circ$ in elastic-plastic material. Results for a direct comparison between the elastic and elasto-plastic material in case of $\theta=45^\circ$ show that extrusions begin to increase much earlier when assuming elasto-plastic material than elastic material, and the magnitudes of extrusion in the elasto-plastic model are significantly higher, as tunnel face approaches the weak ground, due to elasto-plastic yielding near to tunnel face.

From the results for a comparison between $\theta=45^\circ$ and 90° in elasto-plastic material, it is worth noting that general trends of extrusions are similar regardless of inclination of the transition interface. It means, in these situations, extrusion is more useful indicator to detect the existence of the weak ground and to evaluate the stability of the ground and the tunnel itself than by evaluating the vertical settlements or vector orientation only.

3.8 Non-homogeneity

Numerical simulations were carried out to study the influence of non-homogeneity in a material. Geotechnical properties such as deformation modulus, cohesion and friction angle in a ground do not have a single fixed value but may assume any number of values which can be described as random variables. In other words, geotechnical properties were specified to vary as function of grid position in region 1 and region 2. A Gaussian distribution is used to assign values randomly, with a mean value, μ , and standard deviation, s . In case of the commonly used Gaussian distribution, about 68% of the test values will fall within an interval defined by the mean \pm one standard deviation while approximately 95% of all the test results will fall within the range defined by

the mean \pm two standard deviation. The coefficient of variance, COV, is the ratio of the standard deviation to the mean, i.e. $COV = s/\mu$. E. Hoek (2000) notes that a small uncertainty would typically be represented by a $COV=0.05$ while considerable uncertainty would be indicated by a $COV=0.25$.

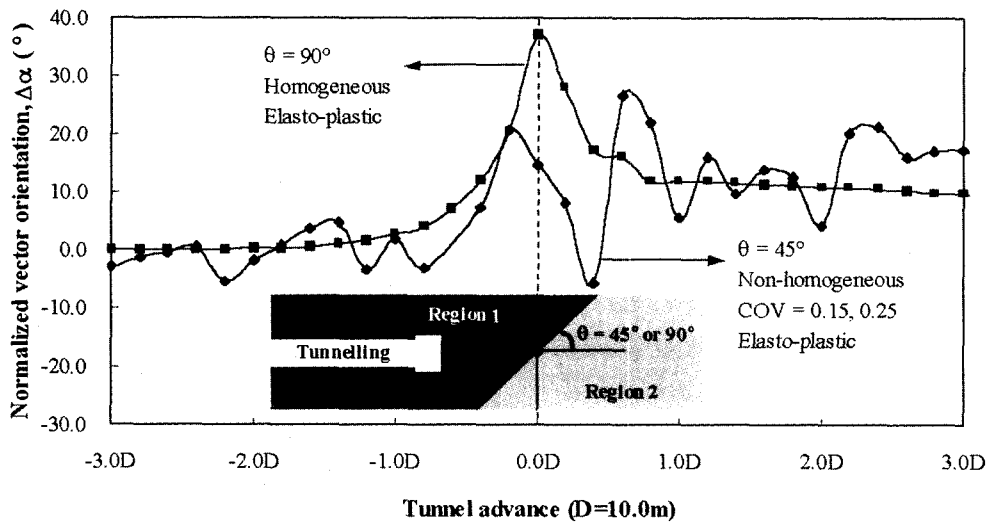
For simulations, the COV were assumed: 0.25 for E_m

and 0.15 for both c and ϕ Table 3 summaries parameters for random input variables with respect to geotechnical properties used in simulations.

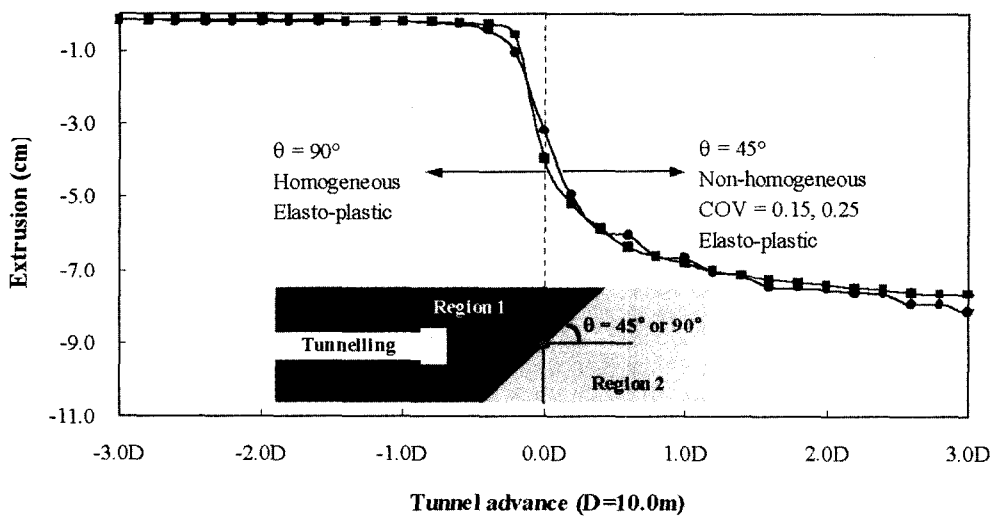
Studies by Steindorfer and Schubert (1997), when tunnelling through the Hinterberg fault zone frequent changes in type and quality of rock caused a number of difficulties in southern Austria, have shown that the

Table 3. Parameters for random input variables

Random variables	Region 1		Region 2	
	Mean, μ_1	Std. deviation, s_1	Mean, μ_2	Std. deviation, s_2
Deformation modulus, E_m (MPa)	1,000	250	100	25
Cohesive strength, c (MPa)	0.3	0.045	0.05	0.0075
Friction angle, ϕ ($^\circ$)	33	5.0	20	3.0



(a) Trends of normalized vector orientation, $\Delta\alpha$



(b) Trends of extrusion at tunnel face

Fig. 16. Trends of vector orientation and extrusion with considering non-homogeneity of the ground in elasto-plastic material assuming that COV for elastic modulus in both region 1 and region 2 is 0.25, and for strength parameters is 0.15

non-homogeneity of the ground frequently led to stress concentration and overloading in zones of stiff area. In addition, these led to a spectacular collapse of the tunnel crown while the conventional evaluation of radial displacement data did not show any significant indication of the failure. In this case history, however, besides a remarkable variation in vector orientation within short distances a general trend could be observed.

As shown in Fig. 16(a), from the results of the vector orientation, there are local variations while a general trend is observed, and beginning of the deviation is not clear to predict the existence of the weak ground. Vector orientation seems to be sensitive to non-homogeneity of the ground and, in this case, other information is necessary to make it clear to predict and evaluate the influence of the weak ground ahead of the tunnel face. As opposed to the results of the vector orientation, trends of extrusion shown in Fig. 16(b) show similar results regardless of the non-homogeneity of the ground.

4. Conclusion

In this paper, detailed three-dimensional numerical study, which explores vertical displacements, vector orientations and extrusions on tunnel face during the progressive advancement for the shallow tunnel in various geotechnical conditions were conducted.

In geodetic methods with 3D data, the measurement of absolute spatial displacements during tunneling has become very common, replacing the previously used convergence measurement. The evaluation of the displacement vector orientation can provide valuable information on changing ground condition ahead of the tunnel face. Thus this method can improve the quality of short term prediction for modifications in excavation and support can be made in time, decreasing the necessity of later reinforcement and repairs. Also, it must be emphasized that because the direction of the longitudinal displacement changes twice in the vicinity of the tunnel face, utmost care about zero reading has to be excised in monitoring and in interpreting monitoring data.

The results, however, of research by numerical study

in this paper showed that in some case displacement vector orientation has shortcomings to predict changing ground condition ahead of the tunnel face. It is important to note that for cases interface of transition at an angle and non-homogeneity of ground, there are local variations. In addition, beginning of the deviation in result of vector orientation is not clear to predict the existence of the weak ground ahead of the tunnel face. Vector orientation seems to be sensitive to non-homogeneity of the ground and inclination of the interface, in this case, and other information is necessary to make it clear to predict and evaluate the influence of the weak ground ahead of the tunnel face.

In those situations, tunnel face extrusion is more useful indicator to detect the existence of the weak ground, and to evaluate the stability of the ground and the tunnel itself than by evaluating the vertical settlements or vector orientation only.

References

1. Ebergardt, E.(2001), "Numerical modelling of three-dimension stress rotation ahead of an advancing tunnel face", *International Journal of Rock Mechanics and Mining Sciences*, 38(4), pp.499-518.
2. Giada, G. and Swoboda, G.(1999), "Developments and applications of the numerical analysis of tunnels in continuous media", *International Journal for Numerical and Analytical Methods in Geomechanics*, 23(13), pp.1393-1405.
3. Golser, H. and Steindorfer, A.(2000), "Displacement Vector Orientations in Tunnelling - What do they tell?", *Felsbau*, 18(2), pp.16-20.
4. Hoek, E. and Brown, E. T.(1997), "Practical estimates of rock mass strength", *International Journal of Rock Mechanics and Mining Sciences*, 34(8), pp.1165-1186.
5. Hoek, E.(2000), "Rock engineering course notes", Rocscience, Toronto, pp.1-313.
6. Itasca(1997), "FLAC3D-Fast Lagrangian Analysis of Continua in 3 Dimensions. Version 2.0. User manual", Minneapolis, Itasca Ltd.
7. Kielbassa, S. and Duddeck, H.(1991), "Stress-strain fields at the tunnelling face - Three-dimensional analysis of two-dimensional technical approach", *Rock Mechanics and Rock Engineering*, 24(3), pp.115-132.
8. Laabmayr, F. and Swoboda, G.(1986), "Grundlagen und entwicklungen bei entwurf und berechnung im seichtligenden tunnel-Teil 1", *Felsbau*, pp.138-143.
9. Lunardi, P. and Focaracci, A.(1999), "The Bologna to Florence high speed railway line: Progress of underground works", *Challenges for 21st Century*, Oslo, pp.585-593.
10. Lunardi, P.(2000), "The design and construction of tunnels using the approach based on the analysis of controlled deformation in rocks and soils", *Tunnels & Tunnelling International*, 32, pp.3-30.

11. Lunardi, P.(2000), "Tunnelling under the Mugello Motor Racing Circuit incorporating the ADECO-RS Approach", *Tunnel*, 8, pp.24-31.
12. Marinos, P. and Hoek, E.(2000), "GSI: A geologically friendly tool for rock mass strength estimation", *GeoEng2000 conference*, Melbourne, Austria.
13. Moritz, B., Vergeiner, R. and Schubert, P.(2002), "Experience Gained at Monitoring of a Shallow Tunnel under a Main Railway Line", *Felsbau*, 20(2), pp.29-42.
14. Pane, X. D. and Hudson, J. A.(1988), "Plane strain analysis in modelling three-dimensional tunnel excavations", *International journal of Rock Mechanics and Mining Sciences & Geomechanics Abstracts*, 25(5), pp.331-337.
15. Panet, M. and Guenot, A.(1982), "Analysis of convergence behind the face of a tunnel", *Tunnelling'82*, London, pp.197-204.
16. Panet, M.(1993), "*Understanding deformations in tunnels*", Pergamon Press, New York, pp.663-690.
17. Rokahr, R. B., Stark, A. and Zachow, R.(2002), "On the Art of Interpreting Measurement Results", *Felsbau*, 20(2), pp.16-21.
18. Schubert, W. and Budil, A.(1995), "The importance of longitudinal deformation in tunnel excavation", *8th Congress on Rock Mechanics: Proceeding of the International Society for Rock Mechanics*, Tokyo, Japan, pp.1411-1414.
19. Schubert, W. and Steindorfer, A.(1998), "Advanced monitoring data evaluation and display for tunnels", *Proc. intern. symp.*, Sao Paulo, pp.1205-1208.
20. Schubert, W., Steindorfer, A. and Button, E. A.(2002), "Displacement Monitoring in Tunnels - an Overview", *Felsbau*, 20(2), pp.7-15.
21. Schweiger, H. and Beer, G.(1996), "Numerical simulation in tunneling", *Felsbau*, 14(2), pp.87-92.
22. Sellner, P. J. and Grossauer, K.(2002), "Prediction of Displacements for Tunnels", *Felsbau*, 20(2), pp.22-28.
23. Steindorfer, A. and Schubert, W.(1997), "Application of new methods of monitoring data analysis for short term prediction in tunneling", *Tunnels for People; Proc. intern. symp.* Wien, Rotterdam: Balkema, pp.65-70.
24. Steindorfer, A.(1998), "*Short term prediction of rock mass behavior in tunnelling by advanced analysis of displacement monitoring data*", Ph.D. thesis, Department of Civil Engineering, Technical University of Graz, Austria, pp.1-111.
25. Tonon, E. and Amadei, B.(2000), "Detection of rock mass weakness ahead of a tunnel - A numerical study", NARMS, In: Girard, Liebman, Breeds and Doe, Seattle, pp.105-111.

(received on Jul. 15, 2003, accepted on Nov. 4, 2003)